WITHDRAWN: Matrix-isolation FT-IR and theoretical investigation of the competitive intramolecular hydrogen bonding in 5-methyl-3-nitro-2-hydroxyacetophenone

ARTICLE *in* JOURNAL OF MOLECULAR STRUCTURE · MAY 2008

Impact Factor: 1.6 · DOI: 10.1016/j.molstruc.2007.12.018

Available online at www.sciencedirect.com
ScienceDirect
Journal of Molecular Structure 880 (2008) 86–96
Journal of MOLECULAR STRUCTURE
www.elsevier.com/locate/molstruc

Matrix-isolation FT-IR and theoretical investigation of the competitive intramolecular hydrogen bonding in 5-methyl-3-nitro-2-hydroxyacetophenone

J. Pajak [a], G. Maes [b], W.M. De Borggraeve [b], N. Boens [b], A. Filarowski [a,*]

[a] Faculty of Chemistry, University of Wroclaw, Joliot-Curie 14, 50-383 Wroclaw, Poland
[b] Department of Chemistry, Katholieke Universiteit Leuven, Celestijnenlaan 200f – bus 02404 3001 Leuven, Belgium

Received 6 September 2007; received in revised form 4 December 2007; accepted 11 December 2007
Available online 25 December 2007

Abstract

The paper presents the conformational, vibrational and hydrogen bond characteristics of 5-methyl-3-nitro-2-hydroxyacetophenone studied with the combined matrix-isolation FT-IR spectroscopic and theoretical (DFT/B3LYP/6-31++G**) technique. Theoretical calculations predict three stable conformations of the studied compound. Only two of these conformations could be identified experimentally using the matrix-isolation FT-IR technique. The conformation with the intramolecular hydrogen bond OH···O=N has been found to be more stable than the conformation with the OH···O=C type of hydrogen bond by 7.28 kJ/mol. The complete assignment of the experimental spectra could be performed based on the theoretical calculations including the normal coordinate analysis and isotopic substitution.

Keywords: *Ortho*-hydroxyacetophenone; Intramolecular H-bonding; Matrix-isolation FT-IR spectroscopy; DFT calculations

1. Introduction

Molecules with intramolecular hydrogen bonding are very often proposed as model systems to study properties of this specific interaction [1,2]. 5-Methyl-3-nitro-2-hydroxyacetophenone is an interesting molecule because it can form two types of intramolecular hydrogen bonding, i.e., the hydroxyl group can either interact with an oxygen atom of the nitro group or with the oxygen atom of the carbonyl group [3]. Both parent molecules of 5-methyl-3-nitro-2-hydroxyacetophenone, *ortho*-hydroxyacetophenone and *ortho*-nitrophenol have been thoroughly studied before by infrared spectroscopy and theoretical calculations [3–6]. Vibrational characteristics of intramolecular hydrogen bonding in *ortho*-nitrophenol have been the topic of numerous experimental and theoretical studies [7–9]. The parameters of the ν_{OH} band in the gas phase, the solution and the solid state have been studied in a wide range of temperatures. It has been stated that the temperature changes of the profile of the ν_{OH} band results mainly from a coupling of this mode with low frequency modes involving stretching and bending vibrations sensitive to intramolecular hydrogen bonding. It also has been shown that in proton accepting solvents, breaking of the intramolecular hydrogen bonding occurs and the formation of intermolecular hydrogen bonding is possible [8,9]. Recently, the experimental spectra of *ortho*-nitrophenol in CCl_4 solution, the solid and the gas phase have been reported in Ref. [10]. A complete vibrational analysis has been performed by using Pulay's DFT-based SQM method. The energetics of the intramolecular hydrogen bonding in *ortho*-nitrophenol has been evaluated by using different approaches [11].

An extensive investigation of the conformational behaviour of several *ortho*-hydroxyphenylalkyl ketones in the solid, liquid and gas phases has been performed in

* Corresponding author. Fax: +48 71 328 2348.
E-mail address: afil@wchuwr.chem.uni.wroc.pl (A. Filarowski).

0022-2860/$ - see front matter © 2007 Elsevier B.V. All rights reserved.
doi:10.1016/j.molstruc.2007.12.019

Ref. [12]. It has been shown that at elevated temperature *ortho*-hydroxyacetophenone can exist in two stable conformations. Further studies dealing with photoisomerization of *ortho*-hydroxyacetophenone isolated in low temperature matrices have provided the first direct spectroscopic observation of its non-intramolecularly hydrogen-bonded rotamer [13]. Theoretical and experimental studies of vibrational properties of *ortho*-hydroxybenzoyl compounds have been performed by Palomar et al. [14]. Using experimental values of the characteristic vibrations of the hydroxyl group, these authors have proposed some empirical equations to evaluate energies of the intramolecular hydrogen bond in *ortho*-hydroxybenzoyl structures. It also has been concluded that the calculated energy of the intramolecular hydrogen bond correlates very well with the spectroscopic parameters of the hydroxyl group, while the vibrations of the C=O group depend mainly on the substituent effect.

Recent crystallographic studies on two derivatives of *ortho*-hydroxyacetophenone (5-chloro-2-hydroxyacetophenone and 3,5-dichloro-2-hydroxyacetophenone) have revealed that substitution of the second chlorine atom to the phenyl ring does not lead to the strengthening of the intramolecular hydrogen bonding [15]. This result was in contrast with the effect observed for *ortho*-hydroxyketimines [16,17].

The solvent effect on the conformational behaviour of 5-methyl-3-nitro-2-hydroxyacetophenone has been evaluated using dipole moment measurements and infrared spectroscopy [3,18].

The objective of the present paper is an investigation of the existence of possible conformations of 5-methyl-3-nitro-2-hydroxyacetophenone in the gas phase using FT-IR matrix-isolation spectroscopy. The experimental studies are combined with detailed theoretical calculations at the DFT(B3LYP) level with the 6-31++G** basis set. A complete vibrational analysis is performed based on the calculated potential energy distribution (PED). The substitution of a hydrogen atom by deuterium in the hydroxyl group permits the identification of the vibrational modes due to the hydrogen bond formation.

2. Experimental

5-Methyl-3-nitro-2-hydroxyacetophenone was purchased from Aldrich Company. High-purity argon gas (N60 = 99.99990%) was obtained from Air Liquide. The experimental equipment used for preparing the matrix samples has been described in detail previously [19,20]. Briefly, the solid compound was evaporated from a home-made mini oven placed in the cryostat. The optimal sublimation temperature was found to be 321 K. The vapour of the product mixed with a large excess of Ar gas was deposited onto a cold CsI window (maintained at 10 K). The IR spectra of the matrices were collected on a Bruker IFS-66 Fourier transform instrument at a resolution of 1 cm^{-1}. Raman spectra of the solid compounds were recorded with a resolution of 4 cm^{-1} on the same instrument equipped with the Raman module FRA 106. The deuterated sample was prepared by dissolving the product in deuterated methanol. The so prepared mixture was refluxed during 20 min. The excess of CH_3OD was removed by evaporation under reduced pressure. This procedure was repeated three times. The deuteration degree was estimated to be ca. 90% by NMR spectra. The ^1H and ^{13}C NMR spectra (spectra not shown) of deuterated samples were recorded in dichloromethane (CD_2Cl_2) solution using a Bruker 500 XL spectrometer.

The geometries of the studied structures were optimized using the DFT method with the hybrid B3LYP functional [21,22] and the 6-31++G** basis set. The IR frequencies and intensities and Raman activities were computed at the same level of theory using the harmonic approximation and the analytical derivative procedure incorporated in the Gaussian 98 program [23]. Based on these results the potential energy distribution (PED) analysis was performed. Theoretically predicted frequencies have been scaled down by applying two scaling procedures. Either all frequencies were scaled with a uniform scaling factor of 0.970 or a set of variable scaling factors was used, depending on the different types of vibrational modes, i.e., 0.950 for ν(XH), 0.980 for the out of plane modes and 0.975 for all others modes. The use of different scaling factors for frequencies has been proposed by several authors in the past [24–27].

3. Results and discussion

3.1. Conformational characteristics

Theoretical calculations predict three stable conformations of 3-methyl-5-nitro-2-hydroxyacetophenone, which are shown in Fig. 1. The total and relative energies and the dipole moments of the three conformations are presented in Table 1. The studied compound can form two types of hydrogen bonding, i.e., the hydroxyl group interacts either with an oxygen atom of the nitro group or the carbonyl oxygen atom of the acetyl group. In the most stable conformation (I), an intramolecular hydrogen bond exist between the hydroxyl group and one of the oxygen atoms of the nitro group: OH···O=N. In this form the methyl group of the acetyl moiety is pointed towards the oxygen atom of hydroxyl group.

The reorientation of the hydroxyl group as well as the acetyl group by 180° results in the formation of another type of intramolecular hydrogen bond OH···O=C, which is present in conformation II. This conformation is 7.28 kJ/mol less stable than conformation I. The nitro group, which is not involved in a hydrogen bond, is turned by 34° out of the plane of the ring. The sterical hindrance between the nitro and hydroxylic oxygen atoms is the reason of this rotation. This conformation, which is the most polar one (μ = 7.75 D), was found to be present in the solid state [28]. In the less stable conformation III the same type

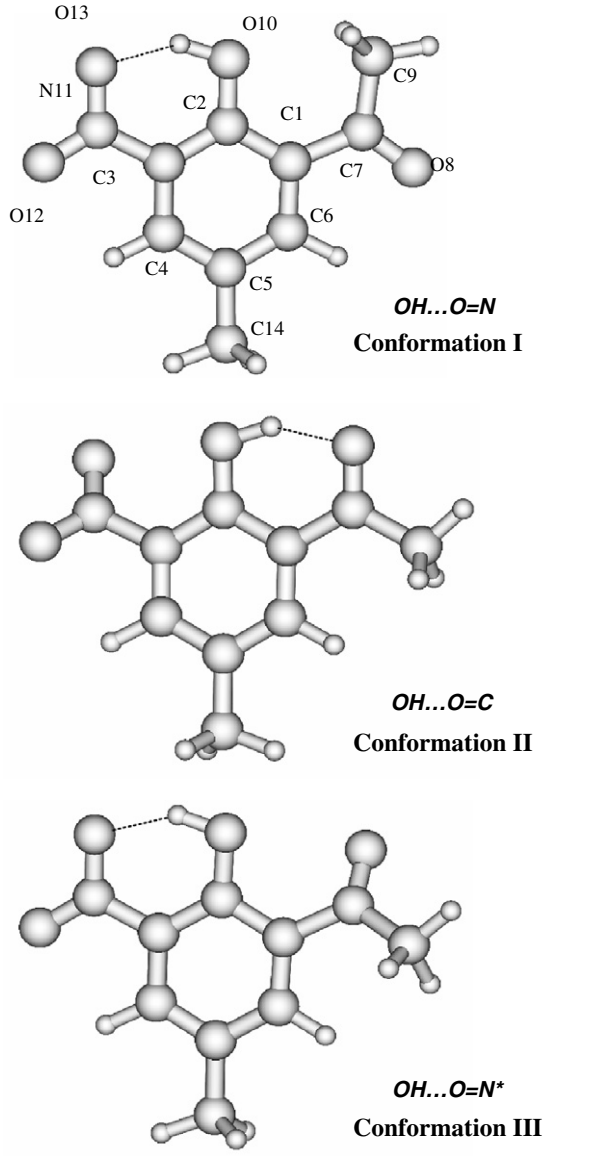

Fig. 1. The optimized geometries of the three stable conformations of 5-methyl-3-nitro-2-hydroxyacetophenone.

Table 1
Total and relative energies and dipole moments of the three stable conformations of 5-methyl-3-nitro-2-hydroxyacetophenone calculated at the DFT(B3LYP)/6-31++G** level of theory

	Conformation I (OH...O=N)	Conformation II (OH...O=C)	Conformation III (OH...O=N)
ΔE (kJ/mol)	0.00	7.28	19.22
μ (D)	1.70	7.75	6.12

of intramolecular hydrogen bond (OH···O=N) exists as in the most stable conformation I. Only the orientation of the acetyl group is different compared to conformation I. The strong repulsion between the oxygen atoms of the hydroxyl and carbonyl group is at the origin of the energy difference (19.22 kJ/mol) with the most stable form.

The values of the calculated relative energies suggest that only conformation I and conformation II will be detectable in the experimental matrix-isolation FT-IR spectrum.

3.2. Vibrational characteristics

The FT-IR spectrum (1750–400 cm^{-1}) of 5-methyl-3-nitro-2-hydroxyacetophenone isolated in Ar is illustrated in Fig. 2. The assignment of almost all the bands in the experimental spectrum was performed using the calculated spectral data for the two most stable conformations of the studied compound. The experimental frequencies (Ar matrix), calculated frequencies, infrared intensities, Raman activities and the mode assignment for conformations I and II are presented in Table 2.

To provide additional support for the assignment of the experimental bands an experiment with the deuterated analogue of the studied compound has been performed. The same frequency region (1750–400 cm^{-1}) of the FT-IR spectrum of the deuterated sample of 5-methyl-3-nitro-2-hydroxyacetophenone isolated in Ar is shown in Fig. 3. The experimental frequencies (Ar matrix), calculated frequencies, infrared intensities, Raman activities and the mode assignment for the isotopically substituted conformations I and II are listed in Table 3.

3.2.1. Vibrations of the OH, C=O and NO_2 groups

The equilibrium between the two conformations is clearly reflected in the IR regions containing the vibrations of the OH, C=O and NO_2 groups [18]. We started the analysis of the spectrum in the region of the ν_{OH} vibration. It has been demonstrated in Ref. [12] that, while the band arising from the stretching vibration of the free hydroxyl group in *ortho*-hydroxyphenylalkyl ketones appears in the range of 3690–3600 cm^{-1}, the vibration of the hydrogen-bonded hydroxyl group in *ortho*-hydroxyacetophenone gives rise to a broad band at 3265 cm^{-1}. Conversely, in the spectrum of *ortho*-nitrophenol, the band located at 3253 cm^{-1} has been assigned to the stretching vibration of the bonded OH group [10]. It is worth noting that the very low intensity of the OH stretching bands [29] is connected with the commonly known phenomenon of so called quasi-aromatic chelate ring [1]. For 5-methyl-3-nitro-2-hydroxyacetophenone the bands arising from the stretching vibrations of the bonded hydroxyl groups in the two conformations cannot be straightforwardly identified in the experimental spectrum because these bands are located in the region of the ν(CH) vibrations. However, the presence of the ν(OH) vibrations in this region can easily be seen from a comparison with the spectrum of a deuterated sample. The broad absorption at 3200–2800 cm^{-1} disappears after deuteration (Fig. 4). Due to overlap with the ν(CH) bands we cannot estimate the position of the ν(OH) bands precisely; only a rough estimation can be given. The profile of the broad band is comparable to that of the band of the ν(OH) vibration in *ortho*-nitrophenol [10]. Therefore, this band is assigned to the ν(OH) mode in the OH···O=N hydrogen bond in conformation I. The

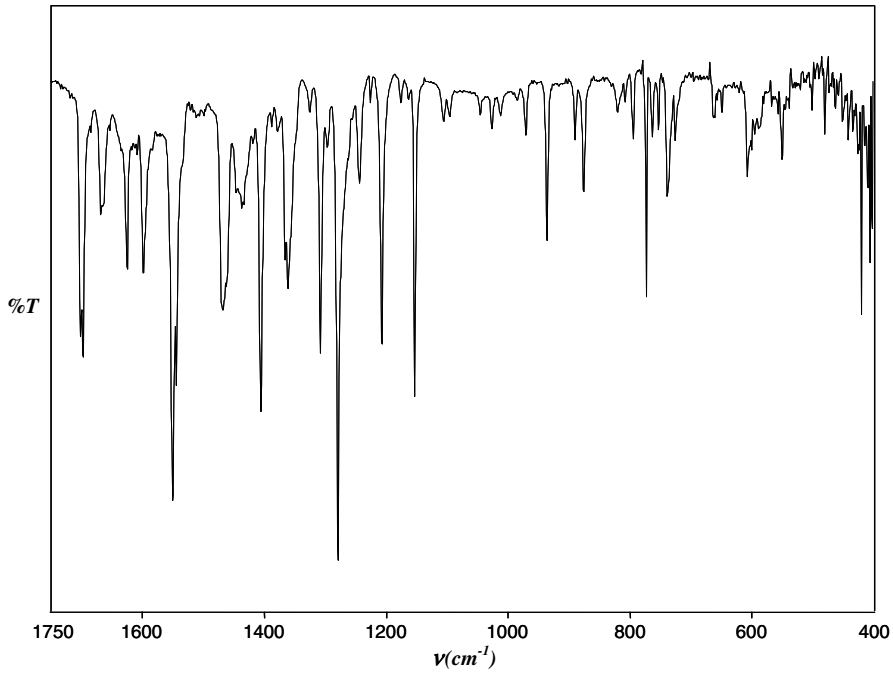

Fig. 2. Matrix FT-IR spectrum of 5-methyl-3-nitro-2-hydroxyacetophenone isolated in Ar (1750–400 cm^{-1}).

frequency of this band can be roughly estimated at 3080 cm^{-1}. After deuteration this band is shifted to 2335 cm^{-1}. From these estimations we calculated an isotopic ratio of 1.32. The band related to the stretching vibration of the hydroxyl group in the OH···O=C type of hydrogen bond is most likely hidden in the right shoulder of the broad band. Its frequency can be roughly estimated at 2900 cm^{-1}. Deuteration shifts the band to 2191 cm^{-1}. Hence, the isotopic ratio also is equal to 1.32.

The experiment with the isotopically substituted compound along with theoretical calculations enabled us to identify the bands of the out-of-plane vibration of the hydroxyl group in the spectrum. This mode gives rise to the bands at 739 and 820 cm^{-1} for conformation I and II, respectively. A relatively large difference between the two theoretically predicted frequencies of the γ(OH) vibrations ($\Delta\gamma(OH) = 76\ cm^{-1}$) is comparable to parameters observable in the experimental spectrum ($\Delta\gamma(OH) = 81\ cm^{-1}$). Complex bands of the γ(OH) vibrations related to two types of hydrogen bonds after deuteration are identified at 530 and 622 cm^{-1} for conformation I and conformation II, respectively.

The existence of two conformations in the matrix is clearly manifested in the region of the C=O stretching vibrations. It has been shown in [30,31], that the ν(C=O) vibration in acetophenone gives rise to a band at 1685 cm^{-1}. Formation of an intramolecular hydrogen bond in *ortho*-hydroxyacetophenone results in shifting this band downwards to 1665 cm^{-1} [12], in agreement with our findings. In the region 1720–1650 cm^{-1}, two intense bands are present, i.e., a very strong doublet at 1701 cm^{-1} and 1696 cm^{-1} due to the stretching vibration of the free carbonyl group in conformation I and a less intense one at 1669/1665 cm^{-1} originating from the vibration of the hydrogen-bonded carbonyl group in conformation II. The latter band is red shifted by 9 cm^{-1} after deuteration. Theoretical calculations reproduce very well both frequencies of the two ν(C=O) bands as well as the isotopic shift value.

The equilibrium between the two forms was also investigated in the region of the $\nu^a(NO_2)$ vibrations. Theoretical calculations predict two bands at 1560 and 1544 cm^{-1} (Table 2), arising from the asymmetric stretching vibration of the hydrogen-bonded and non-hydrogen-bonded (free) nitro group, respectively. This prediction is inconsistent with the experimental results. In the experimental spectra a doublet is observed at 1550/1544 cm^{-1} with a shoulder at 1544 cm^{-1} band. For a correct interpretation of these bands we recorded spectra at different sublimation temperatures (Fig. 5). All the recorded spectra have a doublet at 1550/1544 cm^{-1} and a separate band at 1537 cm^{-1} instead of a shoulder. The intensity of this latter band grows alongside with an increase of sublimation temperature, whereas an opposite picture is observed for the doublet at 1550/1544 cm^{-1} (Fig. 5). Such re-distribution of the intensities results from the equilibrium I⇆II. Verification of the prevailing of one of the conformers are ν(C=O) bands at 1701 cm^{-1} and 1696 cm^{-1}, which refer to conformers I and II, respectively. Assignment of these bands to conformers I and II is properly explained in Ref. [3]. The growing prevalence of conformer I over conformer II causes the increase of the intensity of the band shifted in the direction of the higher frequencies (1701 cm^{-1}) as well as the decrease of the intensity of the band shifted in the direction of low frequencies (1669 cm^{-1}). These observations make it possible to conclude that the doublet at 1550/1544 cm^{-1} (a separate band at low sublimation temperature) is assigned to

Table 2
Experimental (Ar matrix – FT-IR and solid state – Raman) and calculated (B3LYP/6-31++G**) spectral data for conformations I (OH···O=N) and II (OH···O=C)

ν_{exp} IR (cm^{-1})	ν_{cal} [a] (cm^{-1})	ν_{cal} [b] (cm^{-1})	Potential energy distribution[c] conformation I	ν_{exp} IR (cm^{-1})	ν_{cal} [a] (cm^{-1})	ν_{cal} [b] (cm^{-1})	ν_{exp}R (cm^{-1})	Potential energy distribution[c] conformation II
~3080	3209	3143	νO10H(92)		3120	3056	3074	νC4H(99)
3075	3135	3070	νC4H(100)		3107	3043	3059	νC6H(99)
3058	3106	3042	νC6H(100)	~2900	3099	3035		νO10H(90)
3100	3070	3007	$\nu^{d2}CH''_3(74) + \nu^{d1}CH''_3(21)$		3071	3008	3009	$\nu^{d2}CH''_3(71) + \nu^{d1}CH''_3(16) + \nu^{s}CH''_3(12)$
2993	3035	2973	$\nu^{d2}CH'_3(73) + \nu^{d1}CH'_3(19)$		3029	2967	2987	$\nu^{d2}CH'_3(81) + \nu^{d1}CH'_3(14)$
3027	3031	2969	$\nu^{d1}CH''_3(75) + \nu^{d2}CH''_3(25)$		3022	2959		$\nu^{d1}CH''_3(75) + \nu^{d2}CH''_3(25)$
2967	3007	2945	$\nu^{d1}CH'_3(75) + \nu^{d2}CH'_3(25)$		3005	2943	2953	$\nu^{d1}CH'_3(77) + \nu^{d2}CH'_3(19)$
	2967	2906	$\nu^{s}CH''_3(94)$		2959	2898	2928	$\nu^{s}CH''_3(87)$
2939	2952	2891	$\nu^{s}CH'_3(93)$		2950	2889		$\nu^{s}CH'_3(90)$
1701/1696	1695	1703	νC7O8(85)	1669/1665	1651	1659	1651	νC7O8(50)
1624	1614	1622	νC3C4(17) + νC4C5(15) + νC6C1(11)		1615	1623	1614	νC7O8(24) + νC5C6(18) + νC3C4(12)
1598	1580	1588	δO10H(20) + νC5C6(17) + νC2C3(13)	1593/1589	1577	1585	1582	δO10H(21) + νC4C5(20) + νC1C2(13) + νC2C3(10)
1550/1544	1544	1552	$\nu^{a}NO_2(45) + \nu$C4C5(20)	1537	1560	1568	1539	$\nu^{a}NO_2(82)$
[d]	1460	1467	$\delta^{d1}CH'_3(59)$		1467	1474		$\delta^{d2}CH'_3(44) + \delta^{d1}CH'_3(13)$
1468	1458	1465	νC2O10(15) + $\delta^{d1}CH'_3(13) + \nu$C2C3(11) + νC1C2(10)	1462	1451	1459	1456	νC2O10(14) + νC2C3(13)
1446	1446	1454	$\delta^{d2}CH'_3(93)$		1444	1452		$\delta^{d1}CH'_3(72) + \delta^{d2}CH'_3(20)$
1441/1437	1430	1437	$\delta^{d2}CH''_3(93)$		1439	1446		$\delta^{d2}CH''_3(94)$
1428	1415	1423	$\delta^{d1}CH''_3(77)$		1430	1437		$\delta^{d1}CH''_3(79)$
1405	1409	1417	δO10H(24) + νC5C6(15) + $\delta^{d1}CH'_3(13)$		1412	1420		$\delta^{d2}CH'_3(16) + \nu$C5C6(13) + νC6C1(10)
1387	1384	1391	$\delta^{s}CH'_3(93)$	1377	1388	1395		δO10H(22) + δC6H(16) + $\delta^{s}CH'_3(16) + \nu$C3C4(15)
	1374	1382	νC6C1(18) + νC3C4(18) + δO10H(17) + δC6H(13) + δC4H(10)		1381	1388		$\delta^{s}CH'_3(79)$
1350	1358	1365	$\delta^{s}CH''_3(85)$	1366	1360	1367		$\delta^{s}CH''_3(74)$
1308	1306	1312	νC6C1(21) + νC2O10(16) + $\nu^{s}NO_2(16) + \nu$C1C2(11)	1360	1343	1350	1346	$n^{s}NO_2(59) + \delta NO_2(11) + \nu$C3N11(10)
1279	1288	1295	δC4H(17) + δO10H(15) + νC2C3(12) + νC3C4(12)	1325	1314	1321	1313	$\delta^{s}CH''_3(17) + \nu$C1C2(15) + δC1C7O8(13) + νC1C7(10)
1244	1247	1254	νC1C7(15) + $\nu^{s}NO_2(15) + \delta^{1}r(13)$		1296	1303	1279	νC2O10(41) + δC4H(14) + νC3C4(12)
[e]	1246	1253	$\nu^{s}NO_2(21) + \nu$C2O10(21) + δC6H(11)	1273	1262	1268	1269	νC6C1(18) + νC1C7(12) + νC2C3(10)
1207	1193	1199	δC6H(28) + νC5C14(16)	1225	1212	1218		δC6H(37) + νC5C14(16)
1152	1145	1151	δC4H(25) + $\rho^{1}CH''_3(11) + \nu$C2C3(10)		1166	1172	1184	δC4H(36)
1095	1091	1097	$\delta^{1}r(20) + \delta$C6H(14) + δC4H(11)	1105	1087	1093	1107	$\delta^{1}r(19) + \rho^{1}CH''_3(15) + \nu$C1C2(11)
1045	1038	1043	$\rho^{1}CH'_3(73) + \gamma$C5C14(12)		1034	1039		$\rho^{1}CH'_3(63) + \rho^{2}CH'_3(14) + \gamma$C5C14(12)
1027	1018	1023	$\rho^{2}CH''_3(63) + \tau$C1C7O8(18)		1014	1019		$\rho^{2}CH''_3(69) + \tau$C1C7C9(20)
1012	1004	1009	$\rho^{1}CH'_3(68)$		997	1002		$\rho^{2}CH'_3(59) + \rho^{1}CH'_3(13)$
984	969	974	$\rho^{1}CH''_3(36) + \nu$C7C9(15)	971	955	960	982	$\rho^{1}CH''_3(50) + \nu$C7C9(17)
	955	965	γC6H(78) + γC4H(22)		937	942	949	νC5C14(23) + νC3N11(13) + νC5C6(12)
	924	929	νC3N11(13) + νC7C9(12) + νC5C14(11) + νC5C6(11)	935	923	933		γC4H(72) + γC6H(28)

889	882	891	γC4H(78) + γC6H(16)	820	873	882		γO10H(94)
876	8590	864	δNO_2(19) + νC1C7(14) + νC2C3(12) + δ^2r(10)		868	877		γC6H(68) + γC4H(22)
739	797	806	γO10H(100)	876	860	865	876	νC7C9(21) + δNO_2(18) + νC1C7(11)
795	783	787	δ^1r(29) + νC2O10(19) + νC5C14(13) + νC1C2(10)	808	797	801	804	δ^1r(26) + νC2O10(18) + νC1C2(10)
773	745	749	δC1C7(54) + δ^2r(11)	773	760	768		γC2O10(29) + τC3N11O13(21) + γC3N11(16) + τC3N11O12(12)
763	740	748	γC2O10(28) + τC3N11O13(25) + τC3N11O12(15) + τ^1r(13) + γC3N11(12)	753	737	741	754	δNO_2(46)
	708	715	τC3N11O12(28) + τ^1r(19) + γC2O10(19) + τC3N11O13(18) + γC1C7(10)		711	718		γC2O10(20) + τC3N11O12(19) + τ^1r(19) + τC3N11O13(13) + γC1C7(11)
649	639	643	δC2O10(26) + δC3N11O12(14)	661	648	651	664	δC1C7O8(20) + δC2O10(18) + νC7C9(13) + δC3N11O12(10)
607	588	591	δC1C7O8(42) + νC7C9(19) + δC1C7C9(14)	603	592	598	603	τC1C7C9(18) + δC1C7O8(14) + ρ^2CH_3''(11)
594	587	593	τC1C7O8(34) + τ^1r(16) + ρ^2CH_3''(16)	587	574	580	590	τ^1r(19) + δC1C7O8(14)
550	537	543	γC2O10(21) + γC5C14(19) + τ^3r(11)		535	541		τ^1r(22) + γC5C14(11)
	472	475	δ^3r(35) + δC3N11O12(18)		471	474	478	δC3N11O12(12) + νC5C14(10)
	450	452	δC3N11O12(36) + δ^3r(11)		460	462	448	δ^3r(23) + δ^2r(16)
	426	430	τ^2r(37) + γC3N11(21) + τC1C7C9(14)		435	437	417	δ^2r(19) + δC1C7O8(18) + νC1C7(15) + δC2O10 (13)
	415	417	δ^2r(27) + δC5C14(16) + νC3N11(14) + δ^3r(11)		398	402	401	τ^2r(26) + δC3N11O12(14) + τC1C7O8(12) + τ^3r(11)
	372	373	δC2O10(47) + δC3N11(17)		383	385	367	δC1C7C9(19) + δC2O10(15) + δ^3r(15) + νC3N11(11)
	350	352	δC1C7C9(24) + δC1C7O8(16) + νC3N11(11)		350	352		νC1C7(18) + δC2O10(17) + δC1C7(16) + δ^2r(12) + δC5C14(11)
	340	344	γC5C14(34) + γC2O10(23) + τ^1r(20)		323	326	345	γC5C14(35) + τ^1r(20) + γC2O10(13) + δC3N11O12(11) + γC3N11(10)
	322	324	δC1C7C9(33) + νC1C7(28)		303	304	328	δC1C7C9(25) + νC3N11(18) + δC5C14(14) + δ^3r(11)
	226	227	δC5C14(44) + δC3N11(30)		210	211	232	δC5C14(36) + δC1C7(23) + δC3N11(13) + δC1C7C9(11)
	205	207	$\tau CH_3''$(91)		175	176	197	τ^2r(22) + γC3N11(21) + τ^3r(19) + γC1C7(18)
	183	185	τ^2r(40) + γC3N11(30) + γC1C7(16)		173	174		δC3N11(44) + δC1C7(24)
	180	181	δC1C7(62) + δC3N11(17)		151	153		τ^3r(31) + γC5C14(20) + γC1C7(17) + τ^2r(15)
	153	155	τ^3r(24) + γC5C14(23) + τ^2r(14) + γC1C7(12) + γC3N11(11)		136	137		$\tau CH_3''$(95)
	95	96	τC3N11O13(37) + γC2O10(17) + τ^3r(11)		109	110		τC1C7O8(39) + τC1C7C9(21) + γC3N11(18)
	64	65	$\tau CH_3'$(58) + τC3N11O12(16)		62	63		τC1C7C9(30) + τ^3r(20) + τ^2r(12) + γC1C7(11)
	54	55	$\tau CH_3'$(36) + τ^3r(24) + τC3N11O12(18) + τC3N11O13(10)		47	47		$\tau CH_3'$(54) + τC3N11O13(23) + τC3N11O12(19)
	17	18	τC1C7C9(58) + τC1C7O8(37)		45	45		$\tau CH_3'$(39) + τC3N11O12(30) + τC3N11O13(23)

[a] Uniform scaling factor 0.97.
[b] Variable scaling factor: 0.95 for ν(XH); 0.98 for γ and τ; 0.975 for all other modes.
[c] Only contributions $\geqslant$10% are listed: ν-stretching, δ-bending, τ-torsion, γ-out-of-plane motion; r refers to the ring.
[d] Overlap with the band at 1468 cm^{-1}.
[e] Overlap with the band at 1244 cm^{-1}.

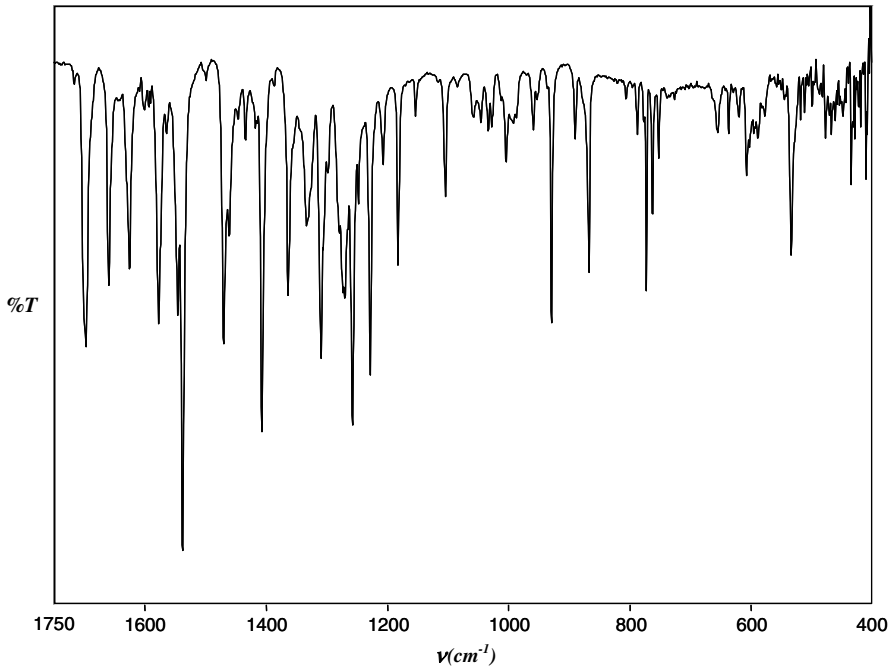

Fig. 3. Matrix FT-IR spectrum of a deuterated sample of 5-methyl-3-nitro-2-hydroxyacetophenone isolated in Ar (1750–400 cm^{-1}).

conformer II. The presented complexities of the bands referring to the nitro group vibrations can be explained by a matrix-site effects. It is interesting that Varsanyi et al. [31] assigned the band arising from the $\nu^a(NO_2)$ vibration in nitrobenzene to the frequency 1548 cm^{-1}. Nearly the same frequency value (1550 cm^{-1}) has been found for the $\nu(NO_2)$ vibration in *ortho*-nitrophenol [10]. This implies that the frequency of the $\nu^a(NO_2)$ mode of a nitro group engaged in an intramolecular hydrogen bond is sensitive to deutero-substitution. It should be noted that both molecules have a planar nitro-phenyl fragment as a consequence of the conjugation between the nitro and the phenyl groups. On the other hand, the theoretical studies on the internal rotation in nitrobenzene have suggested a very small alteration in the conjugation between these two groups [32]. This assumption has been made according to the changes in the Mulliken distribution of the total atomic charges during rotation of the nitro group. Also earlier reports on dipole moment measurements in solution postulated a rather small extent of conjugation in a nitrobenzene molecule [33]. However, investigation of the substituent effect in *ortho*-nitrobenzenes by IR spectroscopy has showed that bands due to the asymmetric and symmetric stretching vibration of a nitro group are slightly shifted towards lower frequency due to the steric effect of bulk substituents [34]. In the case of the studied compound, the steric hindrance between the nitro and hydroxylic oxygen atoms in conformation II results in twisting the nitro group out of the plane of the phenyl ring. As an effect of this rotation, the conjugation of the nitro group to the phenyl ring is reduced and one observes a shift of the $\nu^a(NO_2)$ band to a lower frequency.

The band at 1361 cm^{-1} in the IR spectrum is assigned to symmetric stretching vibrations of the nitro group, which are sensitive to tautomeric equilibrium. This band of middle intensity does not react to deutero-substitution and assigned to conformer II according to DFT calculations (Table 2). However, this band is shifted to the region of low frequencies (1346 cm^{-1}) in the Raman spectrum and to some extent is sensitive to deutero-substitution (1350 cm^{-1}, Table 3), which is described by DFT calculations (1341–1350 cm^{-1}). Such a shift (from 1361 to 1346 cm^{-1}) is evoked by the transition from a non-polar environment (condition of recording of the IR-matrix spectrum) to the solid state (condition of recording of the Raman spectrum). It is interesting that the $\nu^a(NO_2)$ band in the Raman spectrum also is subject to a shift (from 1529 to 1526 cm^{-1}) due to deutero-substitution. The assignment of the $\nu^a(NO_2)$ band (observed in IR spectrum) of conformer I is hindered by a strong coupling with ν(C—O) and ν(C=C) vibrations (1308 and 1244 cm^{-1}, Table 2).

3.3. Vibrations of the CH_3 group

In our previous studies, concerning vibrational analysis of *ortho*-hydroxy aryl *Schiff* bases, we have observed that the deuteration process results not only in the substitution of a hydrogen atom in a hydroxyl group but also in a methyl group attached to the azomethine moiety [35]. Hence, in the present study the theoretical calculations have been performed for a molecule with a deuterium atom substituted in both the hydroxyl and the methyl group of the acetyl moiety. This approach enables us to resolve the very complicated absorption pattern in the ν(CH) vibration region.

In the range of 3330–2800 cm^{-1} (Fig. 4) there are several weak bands present, all overlapping with the broad absorp-

Table 3
Experimental (Ar matrix – FT-IR and solid state – Raman) and calculated (B3LYP/6-31++G**) spectral data for deuterated conformations I (OD···O=N) and II (OD···O=C)

ν_{exp} IR (cm^{-1})	ν_{cal}[a] (cm^{-1})	ν_{cal}[b] (cm^{-1})	Potential energy distribution[c]	ν_{exp}IR (cm^{-1})	ν_{cal}[a] (cm^{-1})	ν_{cal}[b] (cm^{-1})	ν_{exp}R (cm^{-1})	Potential energy distribution[c]
3075	3135	3070	νC4H(100)		3120	3056		νC4H(100)
3058	3106	3042	νC6H(100)		3107	3043		νC6H(100)
2993	3035	2973	$\nu^{d2}CH'_3(73) + \nu^{d1}CH'_3(19)$		3029	2967		$\nu^{d2}CH'_3(81) + \nu^{d1}CH'_3(14)$
2969	3007	2945	$\nu^{d1}CH'_3(75) + \nu^{d2}CH'_3(25)$		3005	2943		$\nu^{d1}CH'_3(77) + \nu^{d2}CH'_3(19)$
2939	2952	2891	$\nu^{s}CH'_3(93)$	2939	2950	2889		$\nu^{s}CH'_3(90)$
~2335	2339	2290	νO10D(93)		2277	2230		$\nu^{d2}CD_3(74) + \nu^{d1}CD_3(20)$
2255	2279	2232	$\nu^{d2}CD_3(74) + \nu^{d1}CD_3(23)$	2191	2262	2215		νO10D(91)
2208	2242	2195	$\nu^{d1}CD_3(75) + \nu^{d2}CD_3(25)$		2236	2190		$\nu^{d1}CD_3(75) + \nu^{d2}CD_3(25)$
	2132	2088	$\nu^{s}CD_3(97)$		2128	2084		$\nu^{s}CD_3(94)$
1697	1691	1699	νC7O8(86)	1660	1640	1649	1643	νC7O8(40)
1624	1611	1619	νC3C4(18) + νC6C1(14) + νC4C5(13)	1574	1612	1620	1616	νC7O8(35) + νC5C6(17)
1577	1556	1564	νC4C5(21) + νC5C6(17) + νC2C3(16) + νC1C2(13)	1546	1562	1570	1568	$\nu^{a}NO_2(63) + \nu$C4C5(11)
1546/1538	1536	1543	$\nu^{a}NO_2(57)$	1537	1543	1551	1526	$\nu^{a}NO_2(21) + \nu$C4C5(17) + νC2C3(13)
1470	1458	1465	$\delta^{d1}CH'_3(26) + \nu$C1C2(13) + νC2O10(12) + $\nu^{a}NO_2(11)$		1461	1468		$\delta^{d2}CH'_3(56) + \delta^{d1}CH'_3(17)$
1457	1455	1463	$\delta^{d1}CH'_3(53)$		1444	1452		$\delta^{d1}CH'_3(72) + \delta^{d2}CH'_3(20)$
1446	1446	1454	$\delta^{d2}CH'_3(93)$	1461	1442	1450	1452/1425	νC1C2(18) + νC2O10(16) + δC6H(15)
1406	1392	1399	νC3C4(17) + νC6C1(15) + $\delta^{s}CH'_3(10) + \delta$C4H(10)	1423	1407	1414		νC3C4(19) + νC6C1(17) + $\delta^{d2}CH'_3(14)$
1387	1383	1390	$\delta^{s}CH'_3(85)$		1382	1389	1389	$\delta^{s}CH'_3(95)$
1333	1326	1333	νC2C3(19) + νC1C2(13) + νC5C6(13) + νC4C5(12)	1361	1350	1357	1350	$\nu^{s}NO_2(57) + \delta NO_2(11)$
1309	1304	1310	$\nu^{s}NO_2(24) + \nu$C2O10(20) + νC6C1(16)	1325	1323	1330	1317	νC1C2(15) + νC1C7(12) + νC5C6(11) + δC1C7O8(11)
1257	1253	1260	δC4H(20) + $\nu^{s}NO_2(18) + \delta^{1}r(12)$		1299	1306	1281	νC2O10(36) + $\nu^{s}NO_2(13) + \nu$C3C4(11)
1247	1247	1254	νC2O10(17) + $\nu^{s}NO_2(15) + \delta$C6H(10)	1273/1261	1264	1270		νC6C1(17) + νC1C7(13) + νC2C3(12) + νC4C5(11)
1227	1216	1223	δC6H(36) + νC5C14(12) + νC3C4(12)		1239	1245		δC6H(41) + δC4H(20)
1181	1165	1171	νC7C9(23) + δC4H(16) + $\delta^{s}CD_3(12) + \nu$C5C14(11)	1207	1194	1200	1214	δC4H(22) + νC5C14(19) + δC6H(10)
1104	1101	1107	$\delta^{1}r(16) + \delta$C4H(16) + δC6H(12) + $\delta^{s}CD_3(12)$	1104	1100	1106	1113	$\delta^{s}CD_3(24) + \delta^{1}r(14) + \nu$C7C9(12) + δC4H(11)
1058	1039	1044	$\delta^{s}CD_3(30) + \delta$O10D(22) + $\delta^{d1}CD_3(12)$	1084	1050	1055		δO10D(32) + $\delta^{s}CD_3(29)$
1045	1038	1043	$\rho^{2}CH'_3(74) + \gamma$C5C14(12)		1038	1043	1043	$\delta^{d2}CD_3(89)$
1033	1031	1036	$\delta^{d2}CD_3(96)$		1034	1039		$\rho^{1}CH'_3(58) + \rho^{2}CH'_3(13) + \gamma$C5C14(10)
1004	1014	1019	$\delta^{d1}CD_3(61) + \delta$O10D(19)		1024	1030		$\delta^{d1}CD_3(90)$
[d]	1006	1011	$\rho^{1}CH'_3(41) + \delta^{d1}CD_3(19)$	[d]	1007	1012		$\rho^{2}CH'_3(40) + \delta$O10D(13)
[d]	991	996	$\rho^{1}CH'_3(27) + \delta^{s}CD_3(18)$		984	989	968	δO10D(17) + $\delta^{s}CD_3(13) + \nu$C4C5(11)
	962	972	γC6H(79)		932	937	947	νC5C14(16) + νC3N11(12) + γC4H(10)
929	923	928	νC5C14(16) + νC3N11(12) + νC5C6(12)		925	935		γC4H(54) + γC6H(31)
	892	902	γC4H(43) + $\rho^{d2}CD_3(26) + \tau$C1C7O8(20)		892	902		$\rho^{2}CD_3(31) + \tau$C1C7C9(26) + γC4H(22)
889	875	884	γC4H(39) + γC6H(20) + $\rho^{2}CD_3(19)$		860	869		γC6H(58) + $\rho^{2}CD_3(14) + \gamma$C4H(12)
867	846	850	$\delta NO_2(20) + \nu$C2C3(14)		846	850	872	$\delta NO_2(22) + \nu$C1C7(12)
	810	814	$\rho^{1}CD_3(49) + \nu$C7C9(12) + δC1C7C9(11)		809	813	802	$\rho^{1}CD_3(22) + \delta^{1}r(17) + \nu$C7C9(13)
787	768	772	$\delta^{1}r(28) + \nu$C2O10(17) + νC5C14(14) + νC7C9(10)		782	786		$\rho^{1}CD_3(27) + \delta^{1}r(11)$
773	740	744	$\delta NO_2(50) + \delta^{2}r(14)$	773	758	765		γC2O10(26) + τC3N11O13(20) + γC3N11(16) + τC3N11O12(11)
763	738	746	τC3N11O13(29) + γC2O10(26) + τC3N11O12(20) + γC3N11(17)	752	731	735	754	$\delta NO_2(42) + \delta^{2}r(13)$
	700	708	$\tau^{1}r(28) + \gamma$C2O10(25) + τC3N11O12(24) + τC3N11O13(13)		702	710		$\tau^{1}r(27) + \gamma$C2O10(23) + τC3N11O12(18) + τC3N11O13(12)

(*continued on next page*)

Table 3 (*continued*)

ν_{exp} IR (cm^{-1})	ν_{cal}[a] (cm^{-1})	ν_{cal}[b] (cm^{-1})	Potential energy distribution[c]	ν_{exp}IR (cm^{-1})	ν_{cal}[a] (cm^{-1})	ν_{cal}[b] (cm^{-1})	ν_{exp}R (cm^{-1})	Potential energy distribution[c]
607	622	625	δC2O10(21) + δC3N11O12(14) + δC3N11(11)	622	637	644		γO10D(76)
~530	581	587	γO10D(100)		621	627	658	γO10D(19) + δC2O10(15) + δC3N11O12(10)
	545	551	τ^1r(41) + γC5C41(21) + τ^3r(11)	578	550	556	588	τ^1r(21) + δC1C7O8(20) + γC5C14(11)
533	538	541	δC1C7O8(41) + νC7C9(20) + ρ^1CD_3(16)		542	548	552	τ^1r(20) + δC1C7O8(14)
	517	522	τC1C7O8(25) + ρ^2CD_3(22) + γC2O10(19) + γC3N11(10)		509	515		ρ^2CD_3(21) + τC1C7C9(16) + γC1C7(11) + γC2O10(10)
	469	472	δ^3r(38) + δC3N11O12(15)		465	467	476	δ^3r(23) + νC5C14(15)
	445	448	δC3N11O12(37) + δ^2r(15)		449	451	446	δC3N11O12(16) + δ^2r(10)
	414	418	τ^2r(32) + γC3N11(18) + τ^3r(16) + τC1C7C9(12)		429	431	417	δ^2r(27) + νC1C7(18)
	413	415	δ^2r(22) + δC5C14(18) + δC3N11O12(13) + νC3N11(12)		391	395	394	τ^2r(27) + τC1C7O8(15) + δC3N11O12(15) + τ^3r(12)
	356	358	δC2O10(40) + δC3N11(18)		371	372		δ^3r(21) + δC1C7C9(16) + νC3N11(15) + δC5C14(11)
	341	343	νC1C7(15) + δC1C7O8(13) + νC1C2(12) + νC3N11(12) + δ^3r(11) + δC2O10(11)		339	340	345	δC2O10(29) + δC1C7(17) + νC1C7(16) + δ^2r(13)
	336	339	γC5C14(33) + γC2O10(23) + τ^1r(21) + τC1C7C9(10)		322	325	325	γC5C14(36) + τ^1r(21) + γC2O10(13) + δC3N11O12(11)
	298	299	δC1C7C9(54) + νC1C7(16)		288	290		δC1C7C9(28) + δC5C14(20) + νC3N11(15)
	225	226	δC5C14(44) + δC3N11(31)		203	204	232	δC5C14(31) + δC3N11(21) + δC1C7(16) + δC1C7C9(14)
	183	185	τ^2r(38) + γC3N11(31) + γC1C7(15) + τ^3r(11)		174	175	197	τ^2r(23) + γC3N11(22) + τ^3r(20) + γC1C7(18)
	173	174	δC1C7(60) + δC3N11(15)		169	170		δC3N11(38) + δC1C7(30)
	155	157	τ^3r(24) + τCD_3(17) + γC5C14(17) + τ^2r(14) + γC1C7(11)		149	151		τ^3r(31) + γC5C14(19) + γC1C7(18) + τ^2r(16)
	144	145	τCD_3(72)		110	111		τC1C7O8(38) + γC3N11(19) + τCD_3(12) + τC1C7C9(11)
	94	95	τC3N11O13(38) + γC1C7(17) + τC3N11O12(10) + τ^1r(10)		95	96		τCD_3(84)
	63	64	$\tau CH_3'$(62) + τC3N11O12(14)		58	59		τC1C7C9(32) + τ^3r(18) + $\tau CH_3'$(12) + γC1C7(11) + τ^2r(11)
	54	55	$\tau CH_3'$(32) + τ^3r(25) + τC3N11O12(18)		47	47		$\tau CH_3'$(49) + τC3N11O13(25) + τC3N11O12(20)
	16	17	τC1C7C9(60)+τC1C7O8(34)		44	44		$\tau CH_3'$(40) + τC3N11O12(28) + τC3N11O13(20)

[a] Uniform scaling factor 0.97.

[b] Variable scaling factor: 0.95 for ν(XD); 0.98 for γ and τ; 0.975 for all other modes.

[c] Only contributions $\geqslant$10% are listed: ν-stretching, δ-bending, τ-torsion, γ-out-of-plane motion; r refers to the ring.

[d] A broad band with few overlapping bands.

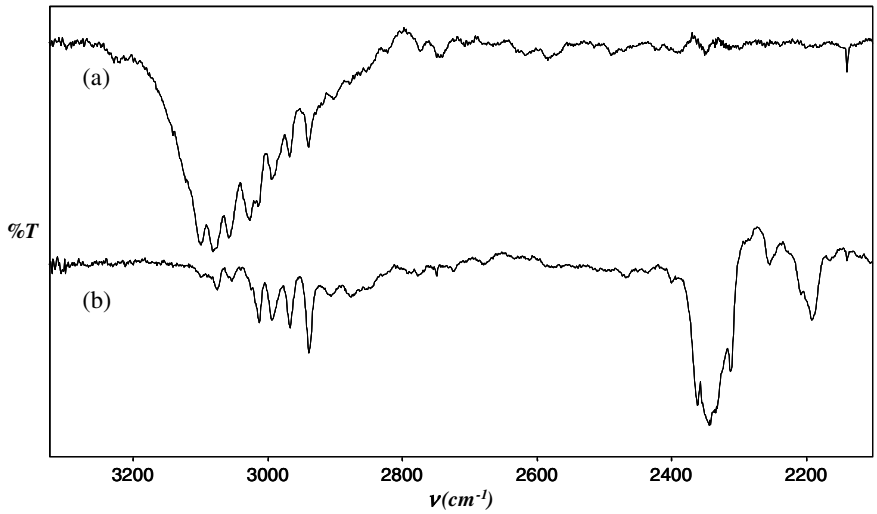

Fig. 4. Matrix FT-IR spectra of 5-methyl-3-nitro-2-hydroxyacetophenone (a) and its deuterated analogue (b), isolated in Ar in the range (3300–2100 cm^{-1}).

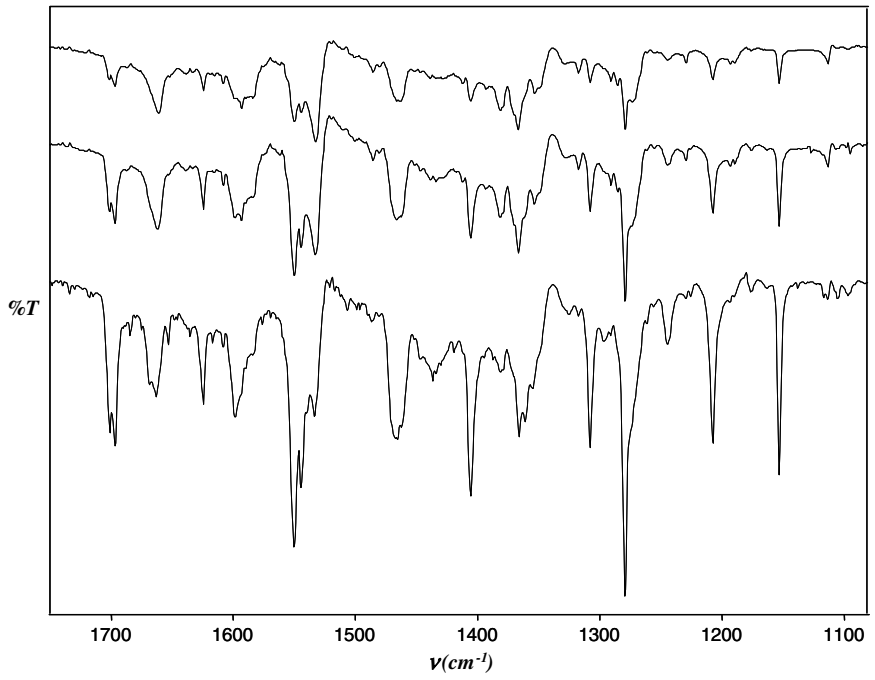

Fig. 5. Matrix FT-IR spectra of 5-methyl-3-nitro-2-hydroxyacetophenone dependent on the sublimation temperature (increase up to down).

tion of the ν(OH) vibrations. The three bands located below 3000 cm^{-1} are assigned to the symmetrical (2939 cm^{-1}) and asymmetrical (2967 and 2993 cm^{-1}) stretching vibration of the 5-methyl group (attached to the benzene ring). Above 3000 cm^{-1} five bands are present, i.e., at 3100, 3075, 3058, 3027 and 3013 cm^{-1}. Two of them (3027 and 3100 cm^{-1}) disappear in the spectrum of the deuterated sample and two new bands appear at 2209 and 2255 cm^{-1}. This enables us to assign these bands to the asymmetrical stretching vibrations of the methyl group in the acetyl moiety. From the theoretical calculation, the intensity of the bands arising from the $\nu^{s}(CH_3)$ vibration is predicted to be very low and this band is experimentally not identifiable. Three other bands (3075, 3013 and 3058 cm^{-1}), not affected upon deuteration, originate from the ν(CH) vibration in the aromatic ring.

The isotopic substitution of the CH_3 group is also clearly seen in the region of $\delta(CH_3)$ and $\rho(CH_3)$ vibrations. The bands at 1441, 1428 and 1350 cm^{-1}, which have been assigned to asymmetrical and symmetrical bending vibration of the methyl group, are located in the spectrum of the deuterated sample in the region of 1058–987 cm^{-1}. In most cases they are coupled with bending vibrations of the OD group and rocking vibrations of the other methyl group. The rocking vibration of the methyl group contributes to the less intense bands at 1027 and 984 cm^{-1}.

The theoretical calculations reproduce very well the changes of the vibrational properties of the methyl group in the acetyl moiety upon isotopic substitution.

4. Conclusions

The combined experimental matrix-isolation FT-IR and theoretical (DFT/B3LYP/6-31++G**) study of the compound 5-methyl-3-nitro-2-hydroxyacetophenone, leads to the following conclusions: (1) Theoretical calculations predict three stable conformations of 5-methyl-3-nitro-2-hydroxyacetophenone. Their relative energy values suggest that only the two most stable of them are observable in the matrix-isolation experimental spectrum. (2) The assignment of almost all bands in the spectrum has been performed using the calculated spectral data and isotopic substitution. (3) The two most stable conformations can be identified in the experimental matrix-isolation spectrum. The conformational equilibrium between the two stable forms is clearly reflected in the region of the C=O and asymmetric NO_2 stretching vibrations. (4) The positions of the ν(OH) bands related to two different types of hydrogen bonds are estimated to be 3090 cm^{-1} for conformation I (OH···O=N) and 2900 $cm^{-1}$for conformation II (OH···O=C). After deuteration the corresponding ν(OD) bands appear at 2335 and 2191 cm^{-1}, respectively. The value of the isotopic ratio for both types of hydrogen bonds is 1.32. (5) As an effect of the rotation of the NO_2 group in conformation II, the conjugation to the phenyl ring is reduced and the $\nu^a(NO_2)$ band is shifted to a lower frequency. (6) The theoretical calculations reproduce very well the changes of the vibrational properties of the CH_3 group in the acetyl moiety upon isotopic substitution.

Acknowledgements

A.F. acknowledges the bilateral collaboration Poland-Flanders (BIL/05/16) and the Wroclaw Centre for Networking and Supercomputing for generous computer time.

References

[1] L. Sobczyk, S. Grabowski, T.M. Krygowski, Chem. Rev. 105 (2005) 3513.
[2] A. Filarowski, J. Phys. Org. Chem. 18 (2005) 686.
[3] A. Konopacka, A. Filarowski, Z. Pawelka, J. Solution Chem. 34 (2005) 929.
[4] H. Lampert, W. Mikenda, A. Karpfen, J. Phys. Chem. 100 (1996) 7418.
[5] A. Simperler, W. Mikenda, Monatsh. Chem. 130 (1999) 1003.
[6] M.V. Vener, S. Scheiner, J. Phys. Chem. 99 (1995) 642.
[7] C.N.R. Rao, Spectroscopy of the nitro group, in: H. Feuer (Ed.), The Chemistry of the Nitro and Nitroso Groups, Wiley, New York, 1969.
[8] V. Schreiber, J. Mol. Struct. 197 (1989) 642.
[9] V. Schreiber, A. Koll, A. Kulbida, I. Majerz, J. Mol. Struct. 348 (1995) 365.
[10] A. Kovasc, V. Izvekov, G. Keresztury, G. Pongor, Chem. Phys. 238 (1998) 231.
[11] G. Buemi, Chem. Phys. 282 (2002) 181.
[12] W.A.L.K. Al-Rashid, M.F. El-Bermani, Spectrochim. Acta A 47 (1990) 35.
[13] E. Orton, M.A. Morgan, G.C. Pimentel, J. Phys. Chem. 94 (1990) 7936.
[14] J. Palomar, J.L.G. De Paz, J. Catalan, Chem. Phys. 246 (1999) 167.
[15] A. Filarowski, A. Koll, A. Kochel, J. Kalenik, P.E. Hansen, J. Mol. Struct. 700 (2004) 67.
[16] A. Filarowski, A. Koll, T. Glowiak, J. Chem. Soc. Perkin Trans. 2 (2002) 835.
[17] A. Filarowski, A. Koll, T. Glowiak, J. Mol. Struct. 615 (2002) 97.
[18] A. Konopacka, Z. Pawelka, J. Phys. Org. Chem. 18 (2005) 1190.
[19] G. Maes, Bull. Soc. Chim. Belg. 90 (1981) 1093.
[20] M. Graindourze, J. Smets, Th. Zeegers-Huyskens, G. Maes, J. Mol. Struct. 222 (1990) 465.
[21] A.D. Becke, J. Chem. Phys. 98 (1993) 5648.
[22] C. Lee, W. Yang, R.G. Parr, Phys. Rev. B 37 (1988) 785.
[23] M.J. Frisch et al., Gaussian 98, Rev A.5 Programme, Gaussian Inc., Pittsburgh, PA, 1998.
[24] M.D. Halls, J. Velkowski, H.B. Schlegel, Theor. Chem. Acc. 105 (2001) 413.
[25] R. Ramaekers, G. Maes, L. Adamowicz, A. Dkhissi, J. Mol. Struct. 560 (2001) 205.
[26] G. Rauhut, P. Pulay, J. Phys. Chem. 99 (1995) 3093.
[27] J. Florian, J. Leszczynski, J. Phys. Chem. 100 (1996) 5578.
[28] A. Filarowski, A. Kochel, A. Koll, G. Bator, S. Mukherjee, J. Mol. Struct. 785 (2006) 7.
[29] A. Filarowski, A. Koll, Vibr. Spectr. 17 (1998) 123.
[30] A. Gambi, S. Giorgianni, A. Passerini, R. Visinoni, S. Ghersetti, Spectrochim. Acta A 36 (1980) 871.
[31] G. Varsanyi, S. Holly, L. Imre, Spectrochim. Acta A 23 (1967) 1205.
[32] V.A. Shlyapochnikov, L.S. Khaikin, O.E. Grikina, C.W. Bock, L.V. Vilkov, J. Mol. Struct. 326 (1994) 1.
[33] V. Vsetecka, O. Exner, Collect. Czech. Chem. Commun. 39 (1974) 1140.
[34] A. Perjessy, D. Rasala, R. Gawinecki, D.W. Boykin, J. Mol. Struct. 382 (1996) 93.
[35] J. Pajak, G. Maes, W.M. De Borggraeve, N. Boens, A. Filarowski, J. Mol. Struct. 844–845 (2007) 83.